

Preparation of Composites from Natural Rubber and Oil Palm Empty Fruit Bunch Cellulose: Effect of Cellulose Morphology on Properties

José Antonio Fiorote,^a Alair Pereira Freire,^a Dasciana de Sousa Rodrigues,^a Maria Alice Martins,^b Larissa Andreani,^a and Leonardo Fonseca Valadares^{a,*}

Rubber tree and oil palm are industrial crops cultivated in the same climate and environment. These plants are used to prepare nanocomposites of natural rubber and cellulose from empty fruit bunches, an abundant residue in the palm oil industry. For this study, the cellulose particles were extracted from the bunches and subjected to enzymatic hydrolysis or microfibrillation to produce nanostructured particles. The nanoparticles were blended with natural rubber latex in an aqueous medium, and the mixture was dried. The properties of the nanocomposites were compared to those of pure natural rubber and unprocessed cellulose composites. The mechanical properties of the natural rubber can be modified by the cellulose content and morphology. As a consequence, it is possible to modulate the material properties by changing only the filler morphology. The use of microfibrillated cellulose had stronger reinforcement effects. The thermal properties of natural rubber were not affected by the addition of cellulose.

Keywords: Composite mechanical properties; Natural rubber; Cellulose fibres nanostructure; Transmission electron microscopy; Oil palm empty fruit bunches

Contact information: a: Embrapa Agroenergy, Parque Estação Biológica S/N, Av. W3 Norte (final), 70770-901, Brasília, DF, Brazil; b: Embrapa Instrumentation, P.O. Box 741, 13560-970 São Carlos, SP, Brazil; *Corresponding author: leonardo.valadares@embrapa.br

INTRODUCTION

Composites and nanocomposites based on renewable resources have attracted great interest due to their environmental friendliness, biocompatibility, and biodegradability (Visakh *et al.* 2012). These two classes are differentiated by the dimensions of the components that constitute the disperse phase of the material (Ray and Okamoto 2003).

Natural rubber (NR) is a renewable polymeric matrix used for the composites and nanocomposite preparations. Natural rubber is a biopolymer with elastic properties derived from latex; it is found in the sapwood of *Hevea brasiliensis* (Bras *et al.* 2010). It is a highly valuable commercial biopolymer used to manufacture industrial and medical products and is essential for the tire and anti-vibration industries (Rolere *et al.* 2016).

Elastomers such as NR can be reinforced by the addition of fillers. Furthermore, an increase in elastic modulus is typically obtained along with a reduction in the strength and elongation of the materials (Angellier *et al.* 2005). Carbon black is commonly used as a filler because of its good interactions with NR (Martins *et al.* 2003). However, due to environmental concerns, reinforcing NR with natural fibres is attractive because they have low density, are readily available, and can be derived from a variety of renewable resources (Dufresne 2006).

Cellulose is a renewable organic material composed of repeating glucose units, and it is one of the main components of plant cell walls. As such, it is the most abundant polysaccharide on Earth and a potential raw material for reinforcing NR composites and nanocomposites. The interactions at the interface of NR and cellulose fibre composites have not been thoroughly explored (Hamed and Li 1977; Flink *et al.* 1988; Yano *et al.* 1992). Yano *et al.* (1992) observed that the orientation of the fibres caused substantial anisotropy in the mechanical properties of composites with higher loadings of cellulose fibres. However, the adhesion between the fibres and the rubber matrix needs improvement. Studies have reported the development of nanocomposites with extracted cellulose nanofibres from different sources (Bendahou *et al.* 2009; Bras *et al.* 2010; Pasquini *et al.* 2010; Siqueira *et al.* 2010; Visakh *et al.* 2012). Generally, formulations with higher nanofibre contents improve Young's moduli and tensile strength. Furthermore, the presence of cellulose nanofibres increase the rate of degradation of the composites in soil (Abraham *et al.* 2012).

Oil palm (*Elaeis guineensis*) and rubber trees are industrial crops that can be cultivated in the same regions of the tropics. During palm oil and kernel oil extraction, a large amount of residual biomass is generated in the form of empty fruit bunches and hulls (Law *et al.* 2007). Palm oil empty fruit bunches can be used to produce long and thin cellulose nanofibres (Fahma *et al.* 2010).

There are different mechanical, chemical, chemo-mechanical and enzymatic methods for obtaining nanostructures from purified cellulose (Visakh *et al.* 2012). In general, cellulose is purified first and then subjected to a controlled hydrolysis process. Under these conditions, the amorphous regions around and between the crystalline cellulose nanofibres preferentially undergo hydrolysis because the hydrolysis kinetics of the amorphous domains are faster than in the crystal region (Silva *et al.* 2009).

The present work described the production of nanostructures from oil palm empty fruit bunches (OPEFB) by mechanical and enzymatic treatments, followed by the preparation of NR composites and nanocomposites using fibres and nanofibres extracted from OPEFB, respectively. The mechanical and thermal properties of those materials was evaluated. The morphology and crystallinity of the fibres and nanofibres were investigated using transmission electron microscopy (TEM) and X-ray diffraction (XRD). The thermal, dynamic mechanical, and mechanical properties of the composites and nanocomposites were evaluated by thermogravimetric analysis (TGA), dynamic mechanical analysis (DMA), and tensile tests.

EXPERIMENTAL

Materials

The centrifuged natural rubber (NR) latex was supplied by QR Borrachas Quirino Ltda (Cedral, Brazil). The latex was collected from RRIM 600 clones in São José do Rio Preto, São Paulo, Brazil, and stabilized with ammonia. The sample presented a dry rubber content of 61.86% and a pH of 9.

The palm oil bunch, belonging to 2301 cultivar Tenera hybrid, was collected in Planaltina, Distrito Federal, Brazil, and autoclaved to remove the fruits.

The following chemicals were used for cellulose purification: ethanol (Vetec, Duque de Caxias, Brazil), petroleum ether (Vetec, Duque de Caxias, Brazil), sodium chlorite (Sigma-Aldrich, St. Louis, USA), and acetic acid (Dinâmica, Indaiatuba, Brazil).

Trichoderma reesei cellulase enzyme (≥ 700 units/g) (Sigma-Aldrich, St. Louis, MO, USA) was used to hydrolyse the cellulose.

Methods

Cellulose purification

The cellulose pulp was obtained as described by Fahma *et al.* (2014) with modifications. The OPEFB were ground using a Willey mill (Fortinox, Piracicaba, Brazil). Accelerated solvent extraction (ASE 350, Dionex, Waltham, MA, USA) was used to remove the extractives with petroleum ether:ethanol (2:1) solution at 105 °C. The resulting material was soaked four times in a sodium chlorite (NaClO_2) solution, acidified to pH 4 with acetic acid, and soaked in 6% potassium hydroxide (KOH) solution for 24 h. The extraction procedures with NaClO_2 and KOH were repeated to ensure the purity of the cellulose. After each extraction, the fibres were sedimented, the supernatant was exchanged for distilled water, and the fibres were stored in an aqueous medium.

Cellulose nanostructure production using enzymatic hydrolysis

Nanostructures were produced by enzymatic hydrolysis of the purified cellulose in a shaker (TE-420, Tecnal, Piracicaba, Brazil) at 5 Hz using cellulase from *Trichoderma reesei* at a concentration of 15 FPU/g for 48 h in a citric acid/sodium citrate buffer solution (pH 5.0) at 50 °C. To inactivate the enzyme and stop the reaction, the sample was heated at 98 °C for 1 h. Finally, the sample was centrifuged and washed with distilled water to remove the buffer and enzymes. The obtained sample was referred to as “hydrolysed cellulose”. The conditions to produce the nanostructures with cellulose were based on preliminary studies.

Microfibrillated cellulose production

To produce the microfibrillated cellulose, the cellulose pulp from the OPEFB was diluted to 1% in distilled water. The dispersion was sheared with an IKA T25 disperser (Staufen, Alemanha) at 24,000 RPM for a total of 120 min. During the shearing process, the temperature and the viscosity of the sample increased, and for this reason, the shearing time was divided in 12 periods of 10 min, and the samples were cooled between the sessions.

Natural rubber/cellulose composite preparation

The composites and nanocomposites were prepared by blending NR latex with purified aqueous cellulose, hydrolysed cellulose nanostructures, or microfibrillated cellulose. The solid contents of the pulp and latex were used to determine the amount of each dispersion required to yield composites with 0.5 per hundred rubber (PHR), 1.0 PHR, 2.5 PHR, or 5.0 PHR. A sample of pure NR was also prepared. The mixtures were stirred for 1 h, poured on glass Petri dishes, and oven-dried at 50 °C for seven days. The samples were dried for one additional day in a vacuum oven.

Characterization

For the TEM analyses, the aqueous dispersion was first diluted and decanted under the action of gravity. Samples were prepared by depositing a droplet of the dispersion on a covered microscope grid (Ted Pella, Redding, CA, USA). After drying, the samples were analysed using a Carl Zeiss TEM 109 microscope (80 kV) (Jena, Germany). Pure cellulose nanostructures and a mixture of cellulose and NR latex (1:1 based on the solid content)

were analysed.

X-ray diffraction measurements were performed in a Shimadzu XRD-6000 diffractometer (Kyoto, Japan) using the reflection mode at a scan rate of 0.5°/min with Cu K α radiation (1.54×10^{-10} m). Purified cellulose, hydrolysed cellulose, and microfibrillated cellulose were freeze dried before the analyses.

Tensile tests were performed using an Arotec WDW-201 universal testing machine (Beijing, China). The specimens were prepared by casting, cut, and then stored at 23 °C in 50% relative humidity for 15 days before the measurements. At least eight specimens were tested for each sample.

The dynamic mechanical properties were measured as a function of temperature using a dynamic mechanical analyser DMA Q800 (TA Instruments, New Castle, USA). The measurements were performed under tension in the temperature range from -120 °C to 120 °C, at a heating rate of 2 °C/min and a frequency of 1 Hz.

Thermogravimetric (TG) analyses were conducted in a Q500 instrument (TA Instruments, New Castle, DE, USA) in the temperature range from 25 °C to 700 °C at a heating rate of 10 °C/min under an inert atmosphere (nitrogen). Approximately 10 mg of sample was used for each analysis.

RESULTS AND DISCUSSION

Typical TEM images of the cellulose after enzymatic hydrolysis are presented in Fig. 1. The cellulose is in the form of needles with size in the micrometer-scale. The isolated fibres presented an average thickness of 6.8 nm with a standard deviation of 2.2 nm based on the measurement of 300 individual particles. The images indicate the fibres were separated, although aggregated particles forced to adhere during water evaporation were also observed.

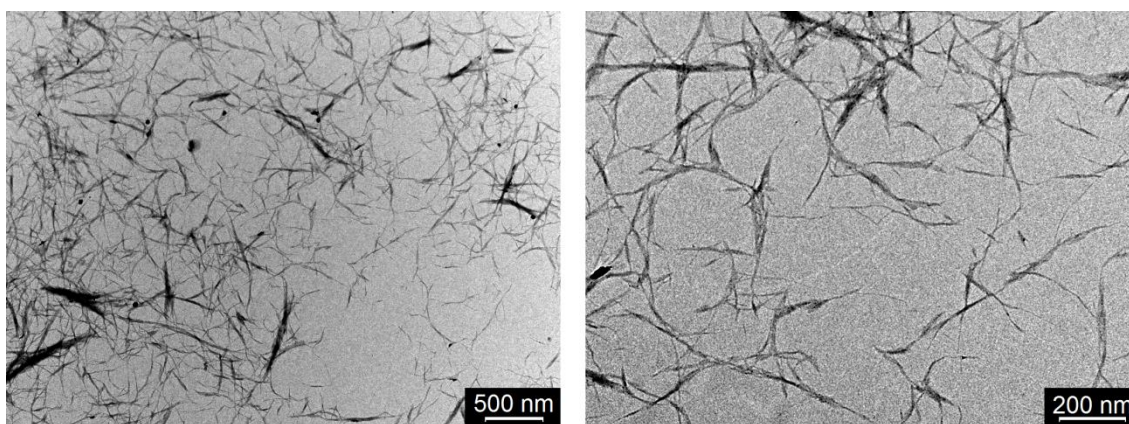


Fig. 1. TEM bright field images of cellulose nanofibres produced by enzymatic hydrolysis of OPEFB

Figure 2 shows the microfibrillated cellulose imaged by TEM. The fibre size and thickness varied extensively, but interconnected fibres ranging from 4 nm to 200 nm were observed. The high shear applied to the cellulose dispersion opened the structures of the cellulose fibres exposing the microfibril structures. No sectioned fibres were observed in the TEM images, indicating that the shear process preferentially disrupted the

intermolecular van der Waals and hydrogen bonds but not the intramolecular covalent bonds along the cellulose chain.

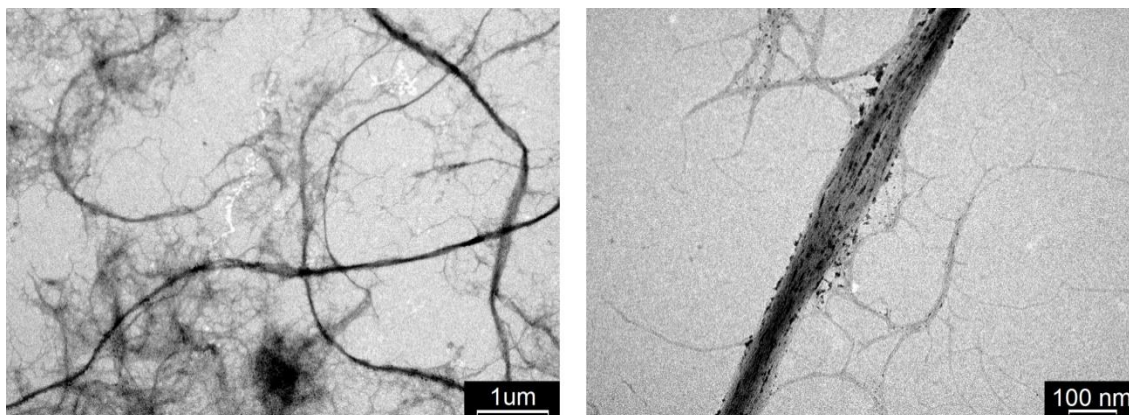


Fig. 2. TEM bright field images of microfibrillated cellulose from OPEFB

The XRD patterns of cellulosic materials are displayed in Fig. 3. The degree of crystallinity was estimated based on the intensity of the crystalline peak and the amorphous halo (Teixeira *et al.* 2010). The following values for the degrees of crystallinity were 38.4% for the empty fruit bunch, 67.9% for the purified cellulose, 47.9% for microfibrillated cellulose, and 60.0% for hydrolyzed cellulose.

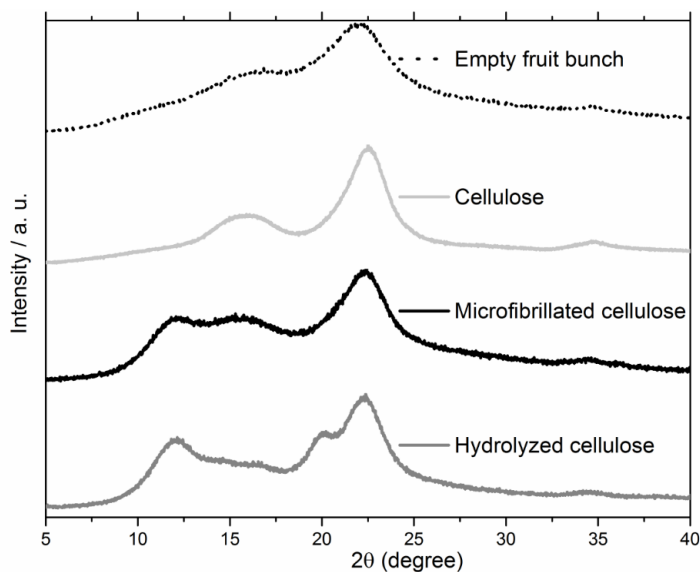


Fig. 3. XRD patterns of OPEFB, cellulose, and their derivatives after mechanical or enzymatic treatments

The low degree of crystallinity was expected for the empty fruit bunch because it contained amorphous materials such as lignin, hemicellulose, and extractives. However, a value of 67.9% was found for purified cellulose. The shear process used to produce the microfibrillated cellulose substantially reduced the material crystallinity. The enzymatic hydrolyses also reduced the cellulose crystallinity, indicating that the enzyme attacked not only the amorphous domains, but also the crystallites.

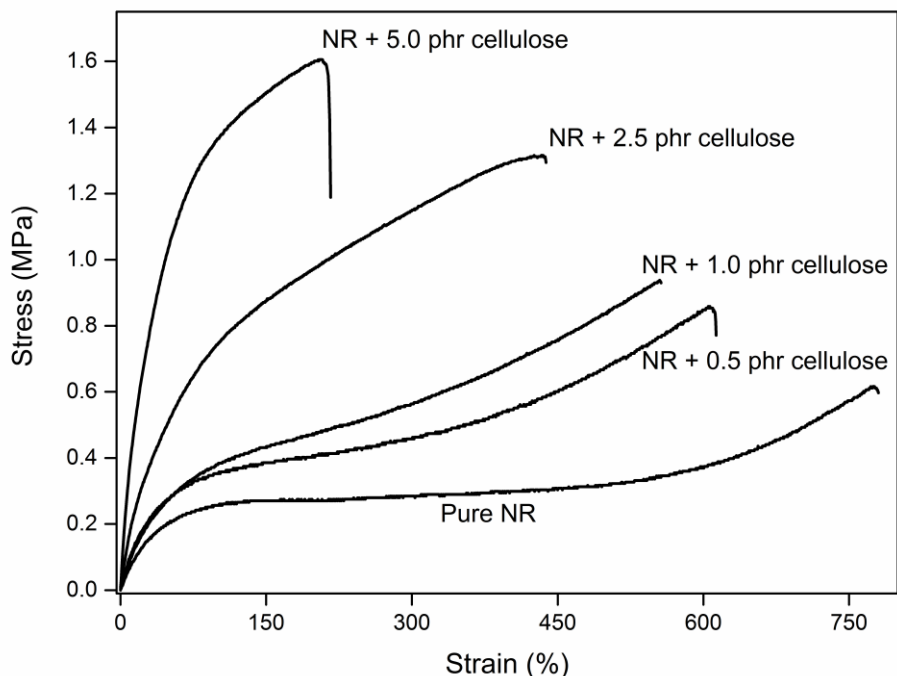


Fig. 4. Stress vs. strain curves for NR and oil palm cellulose-filled composites

Table 1. Mechanical Properties of NR, Composites, and Nanocomposites Filled with Cellulose

Material	Young Modulus (MPa)	Max Strain (%)	Tensile Strength (MPa)
Pure NR	0.528 ± 0.056	784.7 ± 47.8	0.612 ± 0.093
NR + 0.5 PHR cellulose	0.687 ± 0.092	615.4 ± 72.9	0.719 ± 0.112
NR + 1.0 PHR cellulose	0.822 ± 0.047	559.6 ± 42.8	0.922 ± 0.091
NR + 2.5 PHR cellulose	1.659 ± 0.187	434.6 ± 53.1	1.336 ± 0.138
NR + 5.0 PHR cellulose	4.355 ± 0.569	198.9 ± 46.8	1.573 ± 0.142
NR + 1.0 hydrolyzed cellulose	0.672 ± 0.035	806.0 ± 71.1	0.558 ± 0.143
NR + 5.0 hydrolyzed cellulose	1.452 ± 0.148	467.9 ± 29.7	0.694 ± 0.050
NR + 1.0 microfibrillated cellulose	1.005 ± 0.106	504.8 ± 45.1	0.644 ± 0.073
NR + 5.0 microfibrillated cellulose	12.138 ± 1.668	69.6 ± 10.1	1.609 ± 0.139

Note: The errors represent the standard deviation of the measurements.

The tensile test results are presented in Fig. 4 and Table 1. Figure 4 shows representative stress vs. strain curves for the NR and each composite with cellulose. When the weight percentage of cellulose in the composites increased in the range between 0 and 5.0 PHR, the Young's modulus and tensile strength increased as well. However, the maximum elongation decreased with the addition of the cellulose filler. At higher cellulose loads, the samples became more rigid and resistant to the applied external forces. The increased composite strength can be explained by the behaviour of cellulose fibres, which acted as reinforcing filler for the NR. The external force was transferred to the filler and resulted with the material having more traction resistance.

The Young's modulus indicates the specimen's resistance to elastic deformation, which is an indicator of the rigidity of the formed composite. An addition of cellulose to the NR matrix increased the stiffness of the composite. For instance, the pure NR sample presented a Young modulus of 0.528 MPa, while the composite with the addition of 5.0

PHR presented a modulus of 4.355 MPa.

The NR filled with cellulose nanostructures is also a reinforced material, as shown in Fig. 5 and Table 1. The use of microfibrillated cellulose resulted in materials with a higher Young's modulus and tensile strength when compared with pure NR, composite materials, or hydrolysed cellulose nanocomposites. The curve shape of the NR + 5.0 PHR microfibrillated cellulose showed a modulus of 12.138 MPa, a tensile strength of 1.609 MPa, and an elongation of 69.6%.

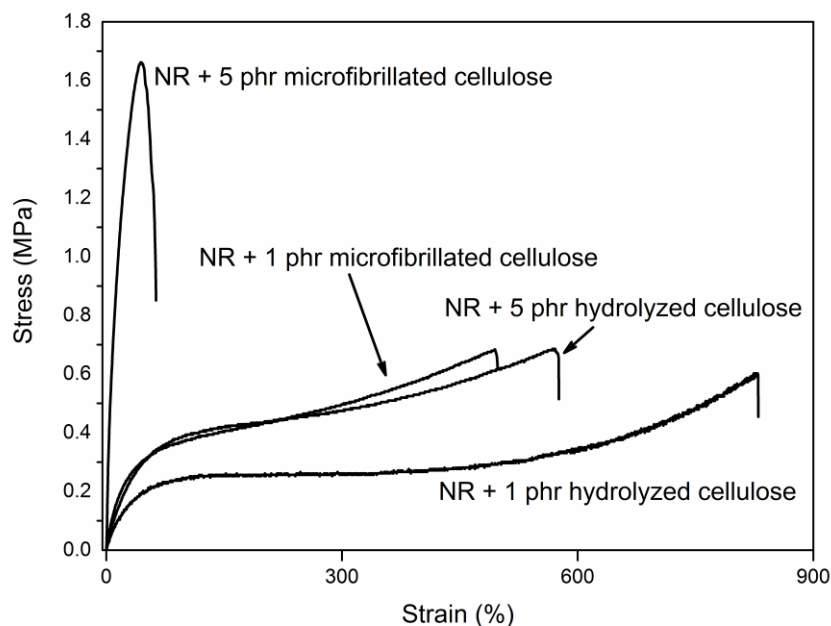


Fig. 5. Stress vs. strain curves for nanocomposites made of NR and cellulose

In order to investigate the effects of cellulose on the dynamics of NR, dynamic mechanical analysis (DMA) was carried out. Figure 6A shows the storage modulus (E'), and Fig. 6B shows the damping factor ($\tan \delta$) as a function of temperature for pure NR, composites, and nanocomposites reinforced with cellulose. The E' indicates the capacity of a material to store the input mechanical energy, and it decreased with temperature in three stages.

At low temperatures, the material in the glassy state exhibited a high modulus. In the second region, which corresponds to the transition from the glassy state to the rubbery state, the modulus decreased sharply as the temperature increased. The maximum value of $\tan \delta$ (Fig. 6B) is attributed to the glass transition temperature (Brazier 1980; Sircar *et al.* 1999). The pure NR presented a T_g of -50 °C. NR + 1.0 PHR cellulose, NR + 1.0 hydrolyzed cellulose, and NR + 5.0 hydrolyzed cellulose presented a T_g of -52 °C. The samples of NR + 5.0 PHR cellulose, NR + 1.0 microfibrillated cellulose, and NR + 5.0 microfibrillated cellulose presented a T_g of -53 °C.

The composites and nanocomposites have lower T_g when compared to pure NR, suggesting the reduction of the dynamics of NR segments with the cellulose addition as a result of interfacial adhesion. The samples prepared with microfibrillated cellulose have the lowest T_g value, which is expected since the microfibrillated cellulose has higher surface area to interact with NR. Overall, the difference of T_g was not great enough to constitute a meaningful difference of thermal behavior among the samples.

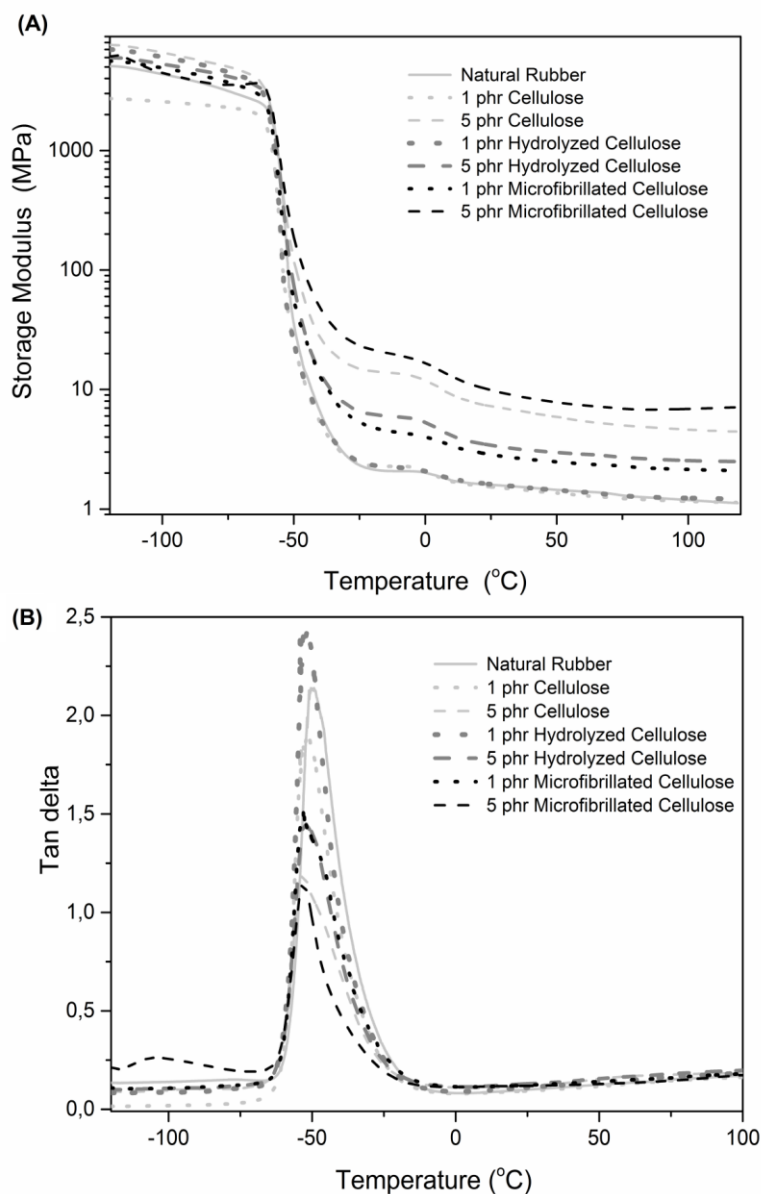


Fig. 6. Dynamic mechanical analysis of NR, composites, and nanocomposites with cellulose. (A) Variation of dynamic storage modulus as a function of temperature. (B) Variation of tan delta as a function of temperature

In the third region, at temperatures above T_g , the values of E' tend to stabilize with increasing temperature, because the materials are in the rubbery state (Benmesli and Riahi 2014). Above T_g , the curves of the samples prepared with 5.0 PHR of filler exhibited the highest values of E' , followed by the nanocomposite with 1.0 PHR of microfibrillated cellulose. The nanocomposite with 1.0 PHR of hydrolysed cellulose and the composite with 1.0 PHR of cellulose had the same behaviour as the NR matrix. The results of storage moduli (Fig. 6A) are in accordance with the Young's moduli measured by tensile tests (Table 1), confirming the reinforcement effect of cellulose. The cellulose content is the main factor to affect the rigidity of the material. Among the composites and nanocomposites with the same cellulose content, the samples prepared with

microfibrillated cellulose have higher moduli.

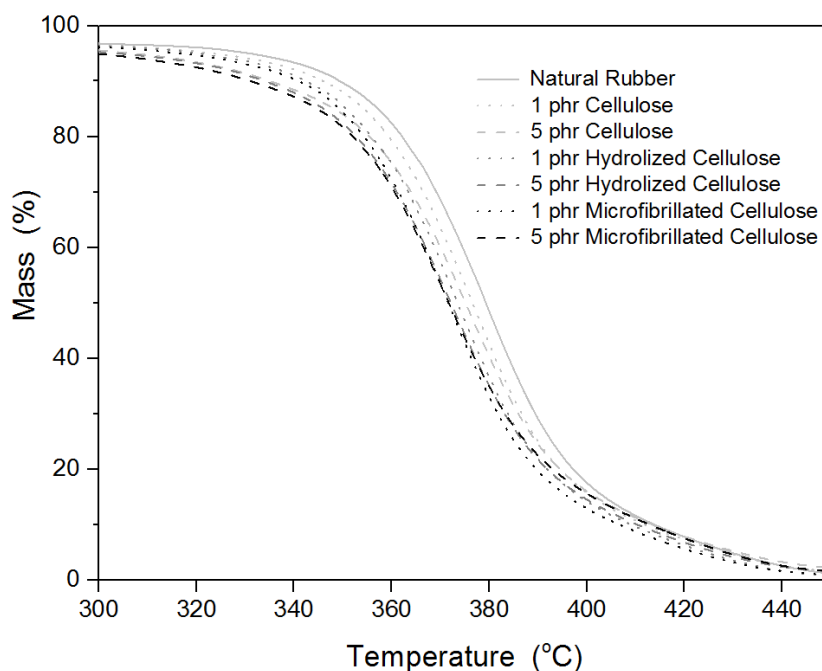


Fig. 7. TGA curves of the NR, composites, and nanocomposites under an inert atmosphere (10 °C/min)

Figure 7 shows the TG curves obtained for the NR composites and nanocomposites in an inert atmosphere. The TG curves of all evaluated samples have the same general shape, suggesting that their decomposition mechanisms were similar. All studied samples exhibited an initial small mass loss, which can be attributed to the elimination of volatile components (de Oliveira *et al.* 2003). The NR, composites, and nanocomposites were stable up to 250 °C, and there were no remarkable differences in the thermal stabilities of the samples up to this temperature, indicating that the addition of various amounts of cellulose did not influence the thermal stability of the materials. The decomposition occurred between approximately 260 °C to 470 °C with a mass loss of approximately 99%, which can be attributed to the thermal decomposition of the cellulose and NR into monomers, dimers, trimers, *etc.*, in an inert atmosphere (Sircar 1997). The temperature of the maximum mass loss rate was approximately 370 °C for all samples. The NR, composites, and nanocomposites underwent almost complete decomposition. At 700 °C, the proportion of residual material was approximately 1.0% for all samples.

Microscopy images of the nanocomposites are presented in Fig. 8 for samples prepared from the NR with (a) hydrolysed cellulose and (b) microfibrillated cellulose. Both samples were prepared by drying mixed aqueous dispersions on a TEM grid. This sample preparation procedure allowed the resulting interactions of the colloidal particles after solvent evaporation to be observed at the microscopic level (Valadares *et al.* 2008).

As shown in Fig. 8A, the cellulose nanoparticles were surrounded by a coalesced polymer matrix, forming agglomerates of NR and hydrolysed cellulose. The fibres appear in light grey tones, and the NR was a grey continuous domain, indicating that the cellulose dispersed within the NR. A polymer surrounding smaller isolated particles was also observed. Diluted microfibrillated cellulose and NR latex can be observed in Fig. 8B, and

the NR colloidal particles adhered to the cellulose which decorated the fibres.

In both cases, Fig. 8 shows that the NR interacted with the cellulose nanostructures. Images show contact between the phases, indicating adhesion at the interface. The interactions with cellulose also deformed the NR particles because they were initially spherical (Rippel *et al.* 2003), as observed by TEM. This result supports the proposed stress transference from the polymer matrix to the filler and the ability of the cellulose to reinforce the NR, as demonstrated by the mechanical tests.

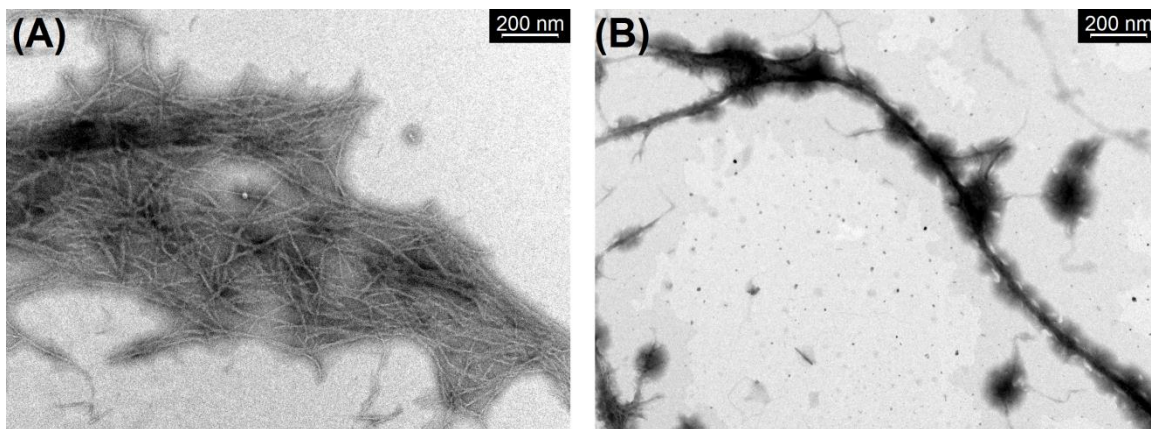


Fig. 8. TEM bright field images of rubber-cellulose clusters formed when a dilute dispersion of latex and cellulose dried over a microscope grid. (a) Sample prepared with NR latex and cellulose nanofibres produced by enzymatic hydrolysis. (b) Samples prepared with NR latex and microfibrillated cellulose

The adhesion of the colloidal particles occurred *via* a sequence of events. First, the particles were confined to smaller volumes and concentrated within the serum ions under water evaporation. Subsequently, the particles were pushed together by capillary forces because of the water's high surface tension (Keddie 1997). After drying, the dissimilar particles adhered due to the intermolecular forces between cellulose and NR.

The adhesion in the dry material was based on intermolecular interactions at the interface. Natural rubber is hydrophobic due to its soluble hydrocarbon chain in nonpolar organic solvents. The NR hydrophobicity was also demonstrated by the ability of carbon black to reinforce this elastomer. Nonetheless, the NR particles were kinetically stable in aqueous latex due to the action of surfactants, such as lipids and proteins, at the surface (Wang *et al.* 2016). In turn, cellulose is considered hydrophilic as it is a carbohydrate with free hydroxyl groups on its chain. However, cellulose is not soluble in water, and it has recently been described as amphiphilic. This behaviour, referred to as the "Lindman hypothesis", has been debated by scientists and used to explain the insolubility of cellulose in most solvents, including water (Glasser *et al.* 2012).

The cellulose amphiphilicity arises from the geometry of the anhydroglucose ring, as observed in crystalline cellulose I. The hydroxyl groups are in equatorial positions laterally along the molecule, allowing them to form hydrogen bonds with parallel chains. In the perpendicular direction, the C-H groups are in axial positions, resulting in the observed hydrophobicity. Therefore, the equatorial direction of the ring is hydrophilic, and the axial direction is hydrophobic.

Many experiments in different research fields have verified the Lindman hypothesis. In this study, the adhesion of cellulose to a hydrophobic phase (NR, shown in

Fig. 8) and load transfer at the interface cannot be explained by the hydrophilicity of cellulose alone.

The morphology of the dispersed phase also accounted for the mechanical behaviour of the resulting material. The use of hydrolysed or microfibrillated cellulose resulted in different changes in various material properties when the same filler content was used. This showed that it is possible to modulate the material properties by changing only the filler morphology. Microfibrillated cellulose was emphasized as a reinforcement agent because its use resulted in a material with a higher Young modulus when compared to the analogous material prepared with conventional fibres or hydrolysed cellulose.

The outstanding reinforcement ability of the microfibrillated cellulose is explained by the large interface area provided by the nanostructure formation during the shear process. The stress transference was only possible due to the interface adhesion, but in this case, the larger surface area allowed greater interactions with the NR. The tension from the microfibrils was transferred to an interconnected network of the cellulose, which stretched and dissipated the force.

CONCLUSIONS

1. The described methodology enabled the preparation of composites and nanocomposites from natural rubber and cellulose presenting higher Young modulus than pure natural rubber (NR).
2. Cellulose nanostructures were extracted from oil palm empty fruit bunches. The enzymatic hydrolysis of the cellulose produced needle-shaped particles, and the microfibrillation process generated a network of interconnected fibres.
3. The mechanical properties of the nanocomposites were modulated as a function of the cellulose content and morphology.
4. The mechanical properties of the NR nanocomposites and cellulose arose from the strong adhesion between the phases.
5. The thermal properties of NR were unaffected by the addition of cellulose, in the range of filler content from 0 to 5 PHR.

ACKNOWLEDGMENTS

The authors acknowledge the Embrapa for financial support (Projeto NanofiBRa – SEG 03.11.07.014.00.00) and colleagues in this corporation: Ana Cláudia Guerra, Rosana Falcão (CENARGEN), Jorge Antonini (CPAC), Raquel Santos de Sousa Ribeiro, Raquel Bombarda Campanha, Thaís Demarchi Mendes (CNPAAE), and José Manoel Marconcini (CNPDIA). The authors thank QR Borrachas Quirino Ltda. for supplying the NR latex.

REFERENCES CITED

- Abraham, E., Elbi, P. A., Deepa, B., Jyotishkumar, P., Pothen, L. A., Narine, S. S., and Thomas, S. (2012). "X-ray diffraction and biodegradation analysis of green composites of natural rubber/nanocellulose," *Polym. Degrad. Stabil.* 97(11), 2378-2387. DOI: 10.1016/j.polymdegradstab.2012.07.028
- Angellier, H., Molina-Boisseau, S., Lebrun, L., and Dufresne, A. (2005). "Mechanical properties of waxy maize starch nanocrystal reinforced natural rubber," *Macromolecules* 38(22), 9161-9170. DOI: 10.1021/ma0512399
- Bendahou, A., Habibi, Y., Kaddami, H., and Dufresne, A. (2009). "Physico-chemical characterization of palm oil from *Phoenix dactylifera* L, preparation of cellulose whiskers and natural rubber-based nanocomposites," *J. Biobased Mater. Bio.* 3(1), 81-90. DOI: 10.1166/jbmb.2009.1011
- Benmesli, S., and Riahi, F. (2014). "Dynamic mechanical and thermal properties of a chemically modified polypropylene/natural rubber thermoplastic elastomer blend," *Polym. Test.* 36, 54-61. DOI: 10.1016/j.polymertesting.2014.03.016
- Bras, J., Hassan, M. L., Bruzesse, C., Hassan, E. A., El-Wakil, N. A., and Dufresne, A. (2010). "Mechanical, barrier, and biodegradability properties of bagasse cellulose whiskers reinforced natural rubber nanocomposites," *Ind. Crop. Prod.* 32(3), 627-633. DOI: 10.1016/j.indcrop.2010.07.018
- Brazier, D. W. (1980). "Applications of thermal analytical procedures in the study of elastomers and elastomer systems," *Rubber Chem. Technol.* 53(3), 437-511. DOI: 10.5254/1.3535051
- De Oliveira, L. C. S., De Arruda, E. J., Da Costa, R. B., Gonçalves, P. S., and Delben, A. (2003). "Evaluation of latex from five hevea clones grown in Sao Paulo State, Brazil," *Thermochim. Acta* 398(1-2), 259-263. DOI:10.1016/S0040-6031(02)00225-3
- Dufresne, A. (2006). "Comparing the mechanical properties of high performances polymer nanocomposites from biological sources," *J. Nanosci. Nanotechnol.* 6(2), 322-330. DOI: 10.1166/jnn.2006.906
- Fahma, F., Iwamoto, S., Hori, N., Iwata, T., and Takemura, A. (2010). "Isolation, preparation, and characterization of nanofibers from oil palm empty-fruit-bunch," *Cellulose* 17(5), 977-985. DOI: 10.1007/s10570-010-9436-4
- Flink, P., Westerlind, B., Rigdahl, M., and Stenberg, B. (1988). "Bonding of untreated cellulose fibers to natural rubber," *J. Appl. Polym. Sci.* 35(8), 2155-2164. DOI: 10.1002/app.1988.070350815
- Glasser, W. G., Atalla, R. H., Blackwell, J., Brown Jr., R. M., Bruchard, W., French, A. D., Klemm, D. O., and Nishiyama, Y. (2012). "About the structure of cellulose: Debating the Lindman hypothesis," *Cellulose* 19(3), 589-598. DOI: 10.1007/s10570-012-9691-7
- Hamed, P., and Li, P. C. (1977). "Reinforcement of EPDM elastomers through discontinuous un-regenerated wood cellulose fibers," *J. Elastom. Plast.* 9, 395-415. DOI: 10.1177/009524437700900405
- Keddie, J. L. (1997). "Latex film formation," *Mater. Sci. Eng.* 21, 101-170. DOI: 10.1016/S0927-796X(97)00011-9
- Law, K. N., Daud, W. R. W., and Ghazali, A. (2007). "Morphological and chemical nature of fiber strands of oil palm empty-fruit-bunch (OPEFB)," *BioResources* 2, 351-362. DOI: 10.15376/biores.2.3.351-362
- Martins, A. F., Suarez, J. C. M., Visconte, L. L. Y., and Nunes, R. C. R. (2003).

- “Mechanical and fractographic behavior of natural rubber-cellulose II composites,” *J. Mater. Sci.* 38, 2415-2422. DOI: 10.1023/A:1023901001185
- Pasquini, D., Teixeira, E.D., Curvelo, A.A.D., Belgacem, M.N., and Dufresne, A. (2010). “Extraction of cellulose whiskers from cassava bagasse and their applications as reinforcing agent in natural rubber,” *Ind. Crops Prod.* 32, 486-490. DOI: 10.1016/j.indcrop.2010.06.022
- Ray, S. S., and Okamoto, M. (2003). “Polymer/layered silicate nanocomposites: A review from preparation to processing,” *Prog. Polym. Sci.* 28, 1539-1641. DOI: 10.1016/j.progpolymsci.2003.08.002
- Rippel, M. M., Lee, L. T., Leite, C. A. P., and Galembeck, F. (2003). “Skim and cream natural rubber particles: Colloidal properties, coalescence and film formation,” *J. Colloid and Interface Sci.* 268(2), 330-340. DOI: 10.1016/j.jcis.2003.07.046.
- Rolere, S., Bottier, C., Vaysse, L., Sainte-Beuve, J., and Bonfils, F. (2016). “Characterization of macrogel composition from industrial natural rubber samples: Influence of proteins on the macrogel crosslink density,” *EXPRESS Polym. Lett.* 10(5), 408-419. DOI: 10.3144/expresspolymlett.2016.38
- Silva, R., Haraguchi, S. K., Muniz, E. C., and Rubira, A. F. (2009). “Applications of lignocellulosic fibers in polymer chemistry and in composites,” *Quim. Nova* 32(3), 661-671. DOI: 10.1590/S0100-40422009000300010
- Siqueira, G., Abdillahi, H., Bras, J., and Dufresne, A. (2010). “High reinforcing capability cellulose nanocrystals extracted from *Syngonanthus nitens* (Capim Dourado),” *Cellulose* 17(2), 289-298. DOI: 10.1007/s10570-009-9384-z
- Sircar, A. K. (1997). “Characterization of isomeric elastomers using thermal analysis,” *J. Therm. Anal.* 49(1), 293-301. DOI: 10.1007/BF01987450
- Sircar, A. K., Galaska, M. L., Rodrigues, S., and Chartoff, R. P. (1999). “Glass transition of elastomers using thermal analysis techniques,” *Rubber Chem. Technol.* 72(3), 513-552. DOI: 10.5254/1.3538816
- Teixeira, E. M., Corrêa, A. C., Manzoli, A., Leite, F. L., Oliveira, C. R., and Mattoso, L. H. C. (2010). “Cellulose nanofibers from white and naturally colored cotton fibers,” *Cellulose* 17, 595-606. DOI: 10.1007/s10570-010-9403-0
- Valadares, L. F., Linares, E. M., Bragança, F. C., and Galembeck, F. (2008). “Electrostatic adhesion of nanosized particles: The cohesive role of water,” *J. Phys. Chem. C.* 112, 8534-8544. DOI: 10.1021/jp710770v
- Visakh, P. M., Thomas, S., Oksman, K., and Mathew, A. P. (2012). “Cellulose nanofibres and cellulose nanowhiskers based natural rubber composites: Diffusion, sorption, and permeation of aromatic organic solvents,” *J. Appl. Polym. Sci.* 124, 1614-1623. DOI: 10.1002/app.35176

- Wang, S., Liu, J., Wu, Y., You, Y., He, J., Zhang, J., Zhang, L., and Dong, Y. (2016). "Micromorphological characterization and label-free quantitation of small rubber particle protein in natural rubber latex," *Anal. Biochem.* 499, 34-42. DOI: 10.1016/j.ab.2016.01.015
- Yano, S., Stenberg, B., and Flink, P. (1992). "Mechanical properties of natural rubber composites reinforced with cellulose fibers," *Nihon Reoroji Gakk.* 20(3), 132-140. DOI: 10.1678/rheology1973.20.3_132

Article submitted: October 22, 2018; Peer review decided: December 15, 2018; Revised version received: December 24, 2019; Updated revised version received and accepted: February 25, 2019; Published: February 27, 2019.
DOI: 10.15376/biores.14.2.3168-3181